Static I-V Characteristics of Optically Controlled GaAs MESFET's with Emphasis on Substrate-induced Effects

Neti V.L. Narasimha Murty and S. Jit

Abstract—**A new analytical model for the static I-V characteristics of GaAs MESFET's under optically controlled conditions in both linear and saturation region is presented in this paper. The novelty of the model lies in characterizing both photovoltaic (external, internal) and photoconductive effects. Deep level traps in the semi insulating GaAs substrate are also included in this model. Finally, effect of backgate voltage on I-V characteristics is explained analytically for the first time in literature. Small signal parameters of GaAs MESFET are derived under both dark and illuminated conditions. Some of the results are compared with reported experimental results to show the validity of the proposed model. Since accurate dc modeling is the key to accurate ac modeling, this model is very useful in the designing of photonic MMIC's and OEIC's using GaAs MESFET.**

Index terms—**Optically controlled GaAs MESFET, photo voltage, deep level traps, backgating, channel length modulation, photonic MMIC's.**

I. INTRODUCTION

Optical control of microwave devices and circuits has been a fertile area of research for the past two decades [1]. In particular, optically controlled GaAs MESFET's (OPFET's) have drawn considerable attention as potential active devices in photonic MMIC's as well as in OEIC's [2-9]. Optical control has many advantages for complex microwave systems such as size reduction, signal isolation, large bandwidth and immunity to electromagnetic interference. With such numerous advantages many potential application like optically controlled amplifiers, oscillators, Light Amplifying Optical Switch (LAOS) and phase shifters, to name a few, become feasible [3-5, 7-9]. The possibility of making use of optical sensitivity of MESFET to form an additional signal input port justifies an increased interest in physical mechanism which occurs when MESFET is illuminated. When photonic MMIC is designed in such a way as to involve the optical phenomenon mentioned above, the circuit designer is immediately aware of the necessity of a good model with all major effects considered. Several researchers experimentally showed that gain, drain current and S-parameters of GaAs MESFET can be controlled by varying incident light on the device in the same manner as varying the gate bias voltage [4, 7-9].

Modeling of I-V characteristics of optically controlled GaAs MESFET has been carried out over the years by several researchers. Salles [7] reported an over simplified analytical model for the I-V characteristics of GaAs MESFET under optically controlled conditions and estimated changes in MESFET small signal parameters due to illumination. Simons [10] derived analytical expressions for I-V characteristics of different types of FET configurations under optical illumination on the devices. He also computed variations in FET small signal parameters such as transconductance, channel conductance with illumination. Singh *et al.* [11] reported an analytical model for the drain-source current of optically controlled GaAs MESFET. They determined the total effective charge in the depletion region below the gate as the summation of the charge

Manuscript received Apr. 23, 2006; revised Jun. 23, 2006.
Center for Research in Microelectronics (CRME),
Department of Electronics Engineering, Institute of Technology, Banaras Hindu University, Varanasi -221005, INDIA
E-mail : nvlnmurty@rediffmail.com, sjit@bhu.ac.in

under dark and additional charge due to the excess holes generated in the depletion region by the incident illumination. However, they did not explain their results in terms of the gate photovoltaic effect and neglected the effect of the photo-generated excess carriers in the active layer of the device. Chakrabarti *et al.* [12] presented an analytical model for the photo-dependent I-V characteristics of GaAs MESFET and explained their results by means of both the excess photo-generated carriers in the depletion region and the photovoltage developed across the Schottky junction. Since, excess holes in the depletion region due to the illumination develop photovoltage across the Schottky junction, inclusion of both these effects (photo-generated excess carriers and photo-induced gate voltage) simultaneously seems to be ambiguous. Further, they also ignored the effect of excess photo-generated carriers in the neutral region. Moreover, the resultant model was very complex as compared to Singh *et al.* [11]. Kawasaki *et al.* [4] demonstrated an illuminated FET model by including an illumination intensity parameter in the *modified Statz* model with a large number of unknown fitting parameters to be extracted either from extensive experimental or from simulation results. Some two-dimensional numerical models of optically controlled GaAs MESFET's are also reported in the literature [13]. Even though, these 2-D models give a good insight into the operation of semiconductor devices, such a modeling is computationally inefficient for RF circuit simulations since behavior of device is strongly influenced by different properties that can change from process to process. However, all of the above models are restricted only for the linear region of operation of the device. Further, none of the above models included the effects of deep level traps in the substrate and backgating.

A slight excess of As in melt during LEC growth of GaAs substrate favors the formation of native EL2 defects which acts as a deep donors (typically with a concentration of 1-2x10^{22} m^{-3}) in GaAs that compensates residual shallow acceptors and makes the substrate semi-insulating [14-15]. These EL2 sites have a tendency to capture some of the free electrons from the channel making the substrate side negatively charged. Hence from the charge balance a positive charge is formed in the channel that pinches off the channel from the backside. Further more, negative bias applied to a nearby electrode can modulate this depletion region causing unwanted coupling among devices on the same wafer. This undesirable phenomenon is called backgating that limits the integration scale of devices in an IC [14-16]. Generally speaking, physical models are highly inefficient because of the lack of unified characterization tools leads to insufficient input data which is crucial to any physical model. Thing goes even worse when comparing device characteristics from process to process in a foundry and from foundry to foundry. Stoneham *et al.* [17] quantitatively compared various device characteristics such as bias dependence of transconductance of FET's and found wide spread out in the device characteristics from one foundry's process to another's. They related backgating (or sidegating) as one of the possible sources of some of these discrepancies. So it has to be well characterized and taken into account in order to apply a physical model to devices fabricated in varieties of foundries. Unfortunately, none of the previous models have included deep level traps and backgating in their models which extremely limits the usage of these models particularly in monolithic IC's.

In this paper we present an analytical modeling of static I-V characteristics of optically controlled GaAs MESFET's in both linear and saturation regions of operation. A comprehensive analytical characterization of photo induced voltages (both internal and external) and photoconductive current in the channel is presented. Deep level traps in the semi insulating substrate as well as in the active layer are considered through which the important effect, backgating is analytically modeled for the first time in the literature under illuminated conditions. In linear region gradual channel approxi mation is used and in saturation region channel length modulation is considered as a source of finite output conductance. Later, small signal parameters of GaAs MESFET under optically controlled conditions are derived from the static I-V characteristics. Finally, some of the results are compared with the reported experimental results to show the validity of the present model. Since accurate dc modeling is the key to accurate ac modeling as well as to complicated microwave characterization, this model is very useful in designing photonic MMIC's and OEIC's with GaAs MESFET as a

basic constituent.

II. THEORETICAL MODEL

The schematic structure of a non-self-aligned GaAs MESFET is shown in Fig 1. Gate area of the device is illuminated with monochromatic light of energy greater than or equal to the band gap energy of GaAs. The metal gate used for the Schottky contact is assumed to be transparent/ semitransparent to the incident light [5, 11-12]. The substrate of the device is assumed to be an undoped high-pure LEC semi-insulating GaAs material. The active channel region of the device is an n-GaAs layer which can be obtained by ion implanting Si into the SI substrate. However, a uniform doping density N_d in the active channel region is assumed. V_{gs}, V_{ds} are the gate-source, drain-source voltages respectively and V_{bg} is the negative voltage applied to backgate to study the backgating effect. In Fig. 1, the depletion region at $y=0$ is a conventional depletion region of Schottky gate and the other depletion region is formed at the channel-substrate interface (at $y=a$) due to the deep level traps in the SI substrate [15, 18]. We call the above two depletion regions as *front* and *back* depletion regions respectively. The widths of these depletion regions are strongly dependent on the substrate properties as well as on the backgate voltage which in turn effects current flowing through the channel. Thus, substrate induced effects are crucial in determining I-V characteristics of the device.

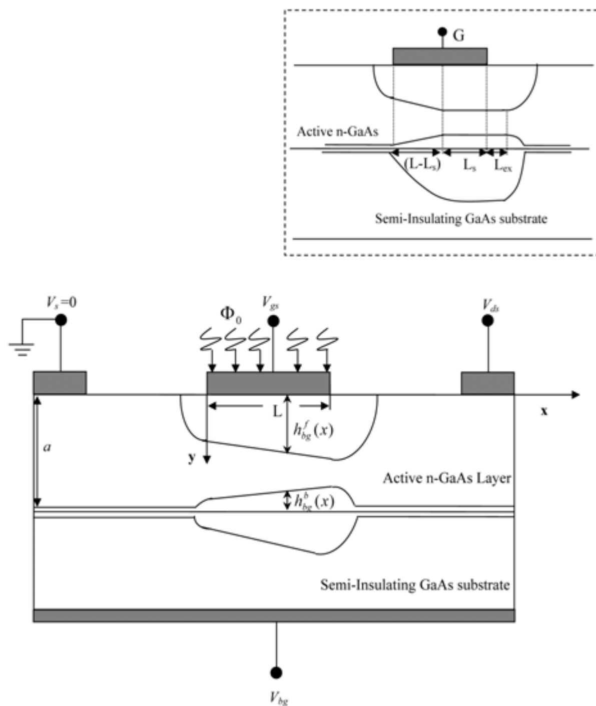

Fig. 1. Schematic diagram of a GaAs MESFET operated in linear region. Φ_0 is photon flux density of the incident radiation. Inset of figure shows shape of depletion regions in saturation region where L_s and L_{ex} are length of velocity saturation regions below and beyond the gate in the channel.

1. Modeling of the Deep Level Traps and Backgating Effects

One method for rendering undoped GaAs wafers semi-insulating is through the careful control of melt stoichiometry during LEC growth. It has been shown that a slight excess of As in the melt favors the formation of EL2 deep donors that compensates residual shallow acceptors (C from B_2O_3 encapsulant) and shallow donors (S or Si) [15].

The probability of an EL2 level to be occupied by an electron in the SI-substrate under thermal equilibrium condition is given by the Fermi function [18]

$$f_{eql}(EL2) = \left\{1 + \frac{1}{g}\exp\left[\frac{(E_T - E_{fs})}{kT}\right]\right\}^{-1} \quad (1)$$

where E_T is energy of the EL2 level, E_{fs} is the Fermi energy level in the substrate bulk, $g(=2)$ is the degeneracy factor of EL2.

The position of Fermi level in the substrate bulk can be obtained from charge neutrality condition in the substrate

$$N^+_{EL2,S} + N^+_{SD} - N^-_{SA} + p_{sub} - n_{sub} = 0 \quad (2)$$

where

$$N^+_{EL2,S} = N_{EL2}\left(1 - f_{eql}(EL2)\right) = N_{EL2}\left\{1 + 2\exp\left[\frac{(E_{fs} - E_T)}{kT}\right]\right\}^{-1}$$

is the density of ionized EL2 traps, n_{sub} , p_{sub} , $N_{SD}^{+} \approx N_{SD}$ and $N_{SA}^{-} \approx N_{SA}$ are the free electron, hole, ionized shallow donor and ionized shallow acceptor concentrations in the bulk substrate under equilibrium condition respectively. Since n_{sub} and p_{sub} are negligibly small as compared to other ionized impurities of Eqn (2), we may write

$$E_C - E_{fs} \approx (E_C - E_T) - kT \ln\left(\frac{N_{EL2} + N_{SD} - N_{SA}}{2(N_{SA} - N_{SD})}\right) \quad (3)$$

the position of the Fermi level E_{fs} is maintained between the intrinsic Fermi level E_i (where $E_C - E_i \approx 0.712\, eV$ at 300 K) and the trap energy level E_T ($\sim 0.689\, eV$ below the conduction band at 300 K) to obtain the semi-insulating nature of the substrate.

Under steady-state non-equilibrium condition, the Fermi statistics described by Eqn (1) becomes invalid. In this case, the Fermi function can be given by

$$f_{non_eql}(EL2) = \frac{e_p + n\,C_n}{e_p + e_n + n\,C_n + p\,C_p} \quad (4)$$

where $C_p = \sigma_p\, v_{pth}$ and $C_n = \sigma_n\, v_{nth}$ are the hole and electron capture coefficients; σ_p and σ_n are the capture cross sections of holes and electrons [18] ; n and p are the free electron and hole concentrations under non-equilibrium condition; v_{pth} and v_{nth} are the thermal velocities of holes and electrons; and e_p, e_n are the emission rates of holes and electrons from EL2 levels respectively [18].

The formation of the back depletion region at the channel-substrate interface is due to the fact that some of the free electrons in the channel gain sufficient energy and enter into the substrate. These electrons are captured by the EL2 traps and a negative space charge region is created at the substrate side [15]. As a result, a depletion region is created at the backside of the channel. The negative charge density accumulated in the substrate can be determined as follows:

Since n and p are negligible in the semi-insulating substrate, the concentration of neutral EL2 states in the substrate side near the channel-substrate (CS) interface under steady-state non-equilibrium condition is given by

$$\begin{aligned} N_{EL2}^{0}(non_eql) &= N_{EL2}\; f_{non_eql}(EL2)\Big|_{n=p\approx 0} \\ &= N_{EL2}\left(\frac{e_p}{e_n + e_p}\right) \end{aligned} \quad (5)$$

the concentration of negative charge in the substrate side of the CS junction is,

$$\begin{aligned} N_{sub}^{-} &= N_{EL2}^{0}(non-eql) - N_{EL2}^{0}(eql) \\ &= \left\{N_{EL2}\left(\frac{e_p}{e_p + e_n}\right)\right\} - \left\{N_{EL2}\left\{1 + \frac{1}{2}\exp\left[\frac{(E_T - E_{fs})}{kT}\right]\right\}^{-1}\right\} \end{aligned} \quad (6)$$

where

$$\begin{aligned} N_{EL2}^{0}(eql) &= N_{EL2}\; f_{eql}(EL2) \\ &= N_{EL2}\left\{1 + \frac{1}{2}\exp\left[\frac{(E_T - E_{fs})}{kT}\right]\right\}^{-1} \end{aligned}$$

is the density of occupied EL2 traps in the bulk substrate under thermal equilibrium condition.

Neglecting the free carrier concentrations in the depletion regions (i.e. $n = p = 0$), the concentration of ionized EL2 states in these depletion regions may be given by

$$N_{EL2}^{+D} \approx N_{EL2}\left(1 - f_{non_eql}(EL2)\Big|_{n=p=0}\right) = N_{EL2}\left(\frac{e_n}{e_n + e_p}\right) \quad (7)$$

assuming that N_d , N_{SD} and N_{SA} are fully ionized in the active layer. The total positive charge concentration in the depletion regions becomes

$$N_{dep}^{+} = N_d + N_{SD} + N_{EL2}^{+D} - N_{SA} \quad (8)$$

a number of experimental and theoretical investigations reported in the literature [16, 19] suggest that there

exists a backgating threshold voltage V_{thbg}, such that if the backgate voltage V_{bg} is below certain threshold voltage V_{thbg}, substrate maintains high resistance with the backgate voltage drops primarily across the bulk substrate and has little effect on the channel thickness. But, when V_{bg} exceeds V_{thbg} (i.e. $V_{bg} > V_{thbg}$), impact ionization of deep traps occurs and the semi insulating substrate transits from a state of high resistivity to low resistivity with the difference $V_{bg} - V_{thbg}$ drops across the CS interface thus widening the back depletion region and narrowing the channel. To include the effect of V_{bg}, voltage across the CS junction for $V_{ds} = 0$ is expressed in the following form

$$V_{ch-s} = \begin{cases} V_{bics}\,; & V_{bg} \le V_{thbg} \\ V_{bics} + \left(V_{bg} - V_{thbg}\right); & V_{bg} > V_{thbg} \end{cases} \tag{9}$$

where V_{bics} is the built-in potential across the channel-substrate junction. Note that the absolute value of the substrate bias V_{bg} is assumed in Eqn (9). Here we have considered V_{thbg} as a parameter without going through details of modeling, details of exact modeling V_{thbg} can be found elsewhere [19].

Wu *et al.* [20] have experimentally demonstrated that the negative voltage applied to a side gate not only modulates the back depletion region at the channel-substrate interface but also modulates the front depletion region below the Schottky gate as if an additional bias is added to the gate. Their study reveals that small portion of gate of MESFET that is in direct contact with substrate further enhances backgating. Hence, any misalignment during photolithography could result in the tip of the gate of the MESFET touching the undoped GaAs thereby enhancing backgating. Since the sidegating and backgating effects are similar to each other, we may also expect similar observation in the case of backgating. We can model the additional voltage $f\left(V_{bg}\right)$ (say) added to the gate as

$$f\left(V_{bg}\right) = \begin{cases} 0\,; & \left|V_{bg}\right| \le V_{thbg} \\ \alpha_1\left(\left|V_{bg}\right| - V_{thbg}\right) + \alpha_2\left(\left|V_{bg}\right| - V_{thbg}\right)^2; & \left|V_{bg}\right| > V_{thbg} \end{cases} \tag{10}$$

where α_1 and α_2 are two empirical constants to be determined from experimental data.

Thus the height of front depletion region at a distance x below the gate including V_{bg} is

$$h_{bg}^{f}(x) = \sqrt{\frac{2\varepsilon_s}{qN_{dep}^{+}}\left(V_{bi} - V_{gs} + f\left(V_{bg}\right) + V(x)\right)} \tag{11}$$

where ε_s is permittivity of GaAs, V_{bi} is built-in potential across Schottky junction and $V(x)$ is the channel potential at any distance x measured with respect to the source.

Similarly, the height of back depletion region measured from channel-substrate interface $\left(y = a\right)$ including backgating can be obtained by solving one dimensional Poisson's equation with appropriate boundary conditions [19]

$$h_{bg}^{b}(x) = \sqrt{\frac{2\varepsilon_s}{qN_{dep}^{+}}\left\{\frac{N_{sub}^{-}}{N_{dep}^{+} + N_{sub}^{-}}\right\}\left(V_{ch-s} + V(x)\right)} \tag{12}$$

Now, the pinch-off voltage of the device may be written as

$$\begin{aligned} V_{po} &= \frac{qN_{dep}^{+}}{2\,\varepsilon_s}\left(a - h_{bg}^{b}(L)\Big|_{V_{ds}=0}\right)^2 \\ &= \frac{qN_{dep}^{+}}{2\,\varepsilon_s}\left(a - \sqrt{\frac{2\varepsilon_s\,V_{ch-s}}{qN_{dep}^{+}}\left\{\frac{N_{sub}^{-}}{N_{dep}^{+} + N_{sub}^{-}}\right\}}\right)^2 \end{aligned} \tag{13}$$

threshold voltage of the MESFET $\left(V_{th}\right)$ including backgating is

$$V_{th} = \left(V_{bi} + f\left(V_{bg}\right)\right) - \left\{\frac{qN_{dep}^{+}}{2\,\varepsilon_s}\left(a - \sqrt{\frac{2\varepsilon_s\,V_{ch-s}}{qN_{dep}^{+}}\left\{\frac{N_{sub}^{-}}{N_{dep}^{+} + N_{sub}^{-}}\right\}}\right)^2\right\} \tag{14}$$

it may be noted that for $N_{EL2} = N_{SD} = N_{SA} = 0$ and $V_{bg} = 0$, the threshold voltage equals to $V_{bi} - \frac{qN_d\,a^2}{2\,\varepsilon_s}$ which is the same as that of the conventional MESFET's [21].

2. Modeling of Photovoltaic Effects

Let Φ_0 be the incident photon flux density (i.e. number of photons per unit area per second) at $y = 0$. Now Φ_0 can be expressed in terms of input optical power as [12]

$$\Phi_0 = \frac{(1 - R_m)(1 - R_s)P_{in}}{h\vartheta\, ZL} \tag{15}$$

where P_{in} is the incident optical power, h is the Planck's constant, ϑ is the frequency of incident light, Z is the width of the gate-metal and R_m and R_s are the reflection coefficients for normal incidence at metal surface and metal-semiconductor interface, respectively. The metal at the gate is assumed to be transparent/ semitransparent to the incident light so that maximum absorption takes place in the sections directly below gate.

Since optical transmission through gate depends on thickness of gate metallization, the metal used for Schottky contact (such as gold) should be made sufficiently thin (~100 Å) to achieve higher transmittance up to 90-95% [5] at the cost of lower unity-gain frequency and higher noise figure. More recently some alternate materials are suggested such as Indium Tin Oxide (ITO) and Al or Ga doped ZnO [22-23]. These thin films are highly degenerate n-type semiconductors with low resistivity. Being wide band gap materials, these are transparent to visible light with transmittance up to 90% in the operating wavelength range $500 - 900$ nm and form good Schottky contact with GaAs [22]. However, we have considered a semi-transparent/transparent gate with transmittance as a parameter (which can be determined by R_m and R_s as defined in Eqn 15) for different metals used for the Schottky contact.

When GaAs MESFET is illuminated with optical radiation on the gate area, absorption of photons takes place in the active channel region as well as in the substrate region of the device. The absorption of light results in the generation of electron-hole pairs in both depletion regions and in the neutral channel. Holes generated in gate-depletion and back-depletion regions are drifted out toward the metal and semi-insulating sides respectively due to the strong electric fields present in depletion regions. Photo-generated excess holes in the neutral channel region are diffused into the front and back depletion regions and are also finally swept out. Further, the photo-generated electrons in the substrate near the channel-substrate junction are also drifted into the active layer of the device. Thus, incident illumination results in two photocurrents: one flows from the active layer to the gate-metal and the other flows from active layer to the semi-insulating substrate. This results in developing photo-voltages across the Schottky junction (i.e. external photovoltage) [7] and the channel-substrate junction (i.e. internal photo voltage) [12]. However, due to the relatively complex structure of the depletion regions of the MESFET, we have assumed that the above induced photo-voltages are independent of the external biasing voltages, which is conformed by several experimental results [8, 13, 24].

i) Derivation of external photovoltage

Let $p^f(y)$ and $p^{ch}(y)$ be the photo-generated hole densities in the front depletion and neutral regions of the channel respectively. Assuming that the excess holes generated in the depletion region are swept out with saturation velocity towards the metal, $p^f(y)$ and $p^{ch}(y)$ may be obtained by solving the following steady state continuity equations [21]:

$$G_{opt} - \frac{p^f(y)}{\tau_p} - v_p \frac{\partial p^f(y)}{\partial y} + \left(D_p \frac{\partial^2 p^f(y)}{\partial y^2} \right) = 0 \tag{16}$$

$$D_p \frac{\partial^2 p^{ch}}{\partial y^2} + G_{opt} - \frac{\left(p^{ch} - p_{no}\right)}{\tau_p} = 0 \tag{17}$$

where $G_{opt} = \Phi_0 \alpha\, e^{-\alpha y}$ is the photo-generation rate of excess carriers, p_{no} is the hole concentration in the active layer under dark condition, $\tau_p \left(= 1/\sigma_p v_{pth} N_{EL2}\right)$ [18], v_p and D_p are the recombination lifetime, saturation velocity and diffusion coefficient of holes respectively. Note that the last term in the left hand side of Eqn (16) has been intentionally introduced to represent the diffusion of excess holes from bulk

towards semiconductor-metal interface to include the surface recombination effect at that interface.

We may solve Eqn (16) using the following boundary conditions [21]:

$$\left.\begin{aligned} & p^f(y = h_o^f) = 0 \\ & D_p \left.\frac{\partial p^f(y)}{\partial y}\right|_{y=0} = S_{pm}\; p^f(0) \end{aligned}\right\} \tag{18}$$

where $S_{pm}\left(=\sigma_p v_{pth} N_{st}\right)$ is the surface recombination velocity of holes at $y = 0$ with surface state density as $N_{st}\left(\approx 1\times 10^{12}\ cm^{-2}\right)$ [18] and $h_o^f = \sqrt{\frac{2\varepsilon_s}{qN_{dep}^+}V_{bi}}$ is the height of Schottky depletion region with no external bias. First boundary condition of Eqn (18) states that excess hole concentration at depletion edge is very small due to the strong fields in the depletion region [21] where as second boundary condition represents the diffusion of excess holes towards the surface and eventual recombination at $y = 0$ [21].

Now the photocurrent due to the excess holes generated in the front depletion region is

$$J_{dep}^f(y)\Big|_{y=0} = qv_p\, p^f(y)\Big|_{y=0} - qD_p \left.\frac{\partial p^f(y)}{\partial y}\right|_{y=0} = qv_p\, p^f(0) - qS_{pm}\, p^f(0) \tag{19}$$

the diffusion current component of excess holes in neutral region can be obtained by solving Eqn (17) with the following boundary conditions [21]

$$\left.\begin{aligned} & \left(p^{ch} - p_{no}\right)\Big|_{y=h_o^f} \approx 0 \\ & \left(p^{ch} - p_{no}\right)\Big|_{y=a-h_o^b} \approx 0 \end{aligned}\right\} \tag{20}$$

where $h_0^b = \sqrt{\frac{2\varepsilon_s}{q\,N_{dep}^+}\left(\frac{N_{sub}^-}{N_{dep}^+ + N_{sub}^-}\right)V_{bics}}$ is back depletion width from $y = a$ into the channel due to the channel- substrate junction under no bias conditions.

From Eqn (17), excess hole density in the neutral channel due to illumination is given by

$$p^{ch}(y) - p_{no} = \frac{\alpha\,\Phi_o \tau_p}{\alpha^2 L_p^2 - 1}\left[\frac{e^{-\alpha h_o^f}}{\xi}\sinh\left(\frac{y - h_o^f}{L_p}\right) - \frac{e^{-\alpha\left(a-h_0^b\right)}}{\xi}\sinh\left(\frac{y-\left(a-h_0^b\right)}{L_p}\right) - e^{-\alpha y}\right] \tag{21}$$

where $\xi = \sinh\left[\frac{h_o^f - \left(a - h_0^b\right)}{L_p}\right]$ and $L_p = \sqrt{D_p \tau_p}$ is the diffusion length of holes.

The resulting photocurrent density flowing from the active layer to the metal due to the diffusion of excess holes generated in the neutral region at depletion edge is

$$J_{diff}^{ch}(h_o^f) = -q\,D_p\left.\left(\frac{\partial p^{ch}(y)}{\partial y}\right)\right|_{y=h_o^f} \tag{22}$$

total photo current density flowing from semiconductor to metal at the gate junction is

$$J_{total} = \left|J_{dep}^f(0)\right| + \left|J_{diff}^{ch}(h_o^f)\right| \tag{23}$$

the photo induced voltage developed across the Schottky junction is [5, 7, 12]

$$V_{op} = \frac{nkT}{q}\ln\left(1 + \frac{J_{total}}{J_s}\right) \tag{24}$$

where n is ideality factor, k is Boltzmann's constant, T is the operating temperature, q is electron charge and J_s is reverse saturation current density of the Schottky junction.

ii) Derivation of internal photovoltage

Since the substrate-depletion region is much larger than that of the back depletion region [15] and the absorption coefficient of GaAs at wavel ength $\lambda \sim 0.83\ \mu m$ is $\alpha \sim 10^6\ m^{-1}$, it may be assumed that for the substrate height $D \sim 10\ \mu m >> 1/\alpha$, most of the absorption take place within the front, back and substrate-depletion regions. Hence optical absorption in the neutral region of the substrate may be neglected. The photo-voltage developed across the channel-substrate junction may be determined as below:

Photo-generated holes in the neutral channel are diffused into the back depletion region as well, diffusion current density at the edge of the back depletion region

may be obtained in a similar manner as considered previously and may be written from Eqn (22)

$$J_{diff}^{ch}(a-h_0^b) = -q D_p \left.\frac{\partial p^{ch}(y)}{\partial y}\right|_{y=a-h_0^b} \tag{25}$$

let $p^b(y)$ be the excess photo generated hole density in the back depletion region. $p^b(y)$ may be obtained by solving

$$v_p \frac{\partial p^b}{\partial y} + \frac{p^b}{\tau_p} - G_{opt} = 0 \tag{26}$$

using boundary condition $\left. p^b \right|_{y=a-h_0^b} \approx 0$ [21]. The solution of Eqn (26) is

$$p^b(y) = \frac{\alpha \Phi_0 \tau_p}{\alpha v_p \tau_p - 1}\left\{\exp\left[-\left(a-h_0^b\right)\left(\alpha - \frac{1}{v_p \tau_p}\right) - \frac{y}{v_p \tau_p}\right] - \exp[-\alpha y]\right\} \tag{27}$$

the hole drift current density at channel-substrate boundary ($y = a$) is thus obtained as

$$J_{dr}^b(y=a) = q v_p p^b(y=a) \tag{28}$$

now, the photo generated electrons in the substrate depletion region are also drifted towards the back depletion region resulting in a photocurrent component flowing from the channel to substrate side. The photo-generated electron density $n^{ss}(y)$ in the substrate-depletion region of channel-substrate junction may be obtained by solving [21]

$$v_n \frac{\partial n^{ss}}{\partial y} + \frac{n^{ss}}{\tau_n} - G_{opt} = 0 \tag{29}$$

where v_n and $\tau_n \left(= 1/\sigma_n v_{nth} N_{EL2}\right)$ are saturation velocity and recombination lifetime of electron in the substrate-depletion region respectively. Using the boundary condition $\left. n^{ss} \right|_{y=a+h_0^{ss}} \approx 0$ [21], we may obtain

$$n^{ss}(y) = \frac{\alpha \Phi_0 \tau_n}{\alpha v_n \tau_n - 1}\left\{\exp\left[-\left(a+h_o^{ss}\right)\left(\alpha - \frac{1}{v_n \tau_n}\right) - \frac{y}{v_v \tau_n}\right] - \exp[-\alpha y]\right\} \tag{30}$$

where

$h_0^{ss} = \left(\frac{N_d}{N_{sub}^-}\right)\sqrt{\frac{2\varepsilon_s}{qN_{dep}^+}\left\{\frac{N_{sub}^-}{N_{dep}^+ + N_{sub}^-}\right\}\left(V_{bics}\right)}$ is the assumed height of the substrate-depletion region from $y = a$ under no bias condition.

The electron drift current density at CS interface flowing from substrate into channel is

$$J_{dr}^{ss}(y=a) = q v_n n^{ss}(y=a) \tag{31}$$

hence, the total photo current density flowing from the active layer to the substrate is

$$J_{total}^{ch-cs} = \left|J_{diff}^{ch}(a-h_o^b)\right| + \left|J_{dr}^b(a)\right| + \left|J_{dr}^{ss}(a)\right| \tag{32}$$

the photo voltage developed across this junction can be written as [12, 24],

$$V_{opcs} = \frac{nkT}{q}\ln\left(1 + \frac{J_{total}^{ch-cs}}{J_s^{ch-cs}}\right) \tag{33}$$

where J_s^{ch-cs} is the reverse saturation current density at channel-substrate junction.

iii) Photo conductive current

Along with photovoltaic effects photoconductive effects in active channel also manifests when the device is illuminated. Overall photo response of the device to optical illumination will be the superposition of both components considering one at a time. In the previous subsections we modeled photovoltaic effects without considering photoconductive effects. In this subsection we tried to quantify photoconductive effects.

Photo generated holes and electrons in the channel due to incident illumination contribute to the photoconductive current in the active region. Associated photoconductive current density can be expressed in terms of these carrier concentrations as

$$J_{pc} = q\left(n^{ch} v_n + p^{ch} v_p\right) \quad (34)$$

where n^{ch} and p^{ch} (Eqn (21)) are photo generated electron and hole concentrations in the channel, v_p and v_n are drift velocities of electrons and holes.

The recombination rates of majority carrier electrons and minority carrier holes in a semiconductor are equal:

$$\frac{n^{ch}}{\tau_n} = \frac{p^{ch}}{\tau_p} \quad (35)$$

associated photoconductive current can be obtained by integrating ZJ_{pc} from $y = h_{bg}^f$ to $y = a - h_{bg}^b$.

$$\therefore I_{pc} = \int_{y=h_{bg}^f}^{y=a-h_{bg}^b} ZJ_{pc}\,dy = Z\int_{y=h_{bg}^f}^{y=a-h_{bg}^b} p^{ch} q\left(\frac{\tau_n}{\tau_p} v_n + v_p\right) dy$$

$$= Zq\left(\frac{\tau_n}{\tau_p} v_n + v_p\right)\int_{y=h_{bg}^f}^{y=a-h_{bg}^b} p^{ch}\,dy$$

in GaAs MESFET's the channel height is in sub-micron regime, diffusion length is several microns (typically 2-10 μm) and the absorption coefficient is in the range $1-4\times10^6$ /m for wavelengths $0.65-0.85$ microns hence it is wise enough to assume $\left(a - h_{bg}^f - h_{bg}^b\right)/L_p << 1$, $\alpha h_{bg}^f << 1$ and $\alpha\left(a - h_{bg}^b\right) << 1$.

Final simplified expression for photoconductive current after several approximations is

$$I_{pc} = 0.5Zq\frac{\alpha^2 \Phi_o \tau_p}{\alpha^2 L_p^2 - 1}\left[\frac{\tau_n}{\tau_p} v_n + v_p\right]\left[a - h_{bg}^f - h_{bg}^b\right]^2 e^{-\alpha h_{bg}^f} \quad (36)$$

it can be seen that photoconductive current is a strong function of gate-source voltage and device parameters. As V_{gs} increases negatively effective channel opening $\left(a - h_{bg}^f - h_{bg}^b\right)$ decreases and photoconductive current also decreases. Due to square dependence of I_{pc} on effective channel opening magnitude of I_{pc} is generally in sub-microampere range.

3. I-V Characteristics of GaAs MESFET under Illumination

De Salles [7] has shown experimentally that if a high resistance ($\geq 50\,k\Omega$) is connected at the gate biasing circuit, photo-voltage developed across Schottky junction is superimposed on gate voltage. The effective gate-source bias under illumination becomes

$$V_{opgs} \approx V_{gs} + V_{op} \quad (37)$$

similarly, the photo-voltage developed across the channel-substrate junction will change the built-in potential across the junction [24]. It was also conformed by 2-D numerical simulations [13]. The effective built-in potential under illuminated condition will be

$$V_{opbi} \approx V_{bics} - V_{opcs} \quad (38)$$

drain-source current of GaAs MESFET under illuminated condition will be the superposition of both photovoltaic and photoconductive effects.

$$I_{ds} = I_{pv} + I_{pc} \quad (39)$$

where I_{ds} is final drain-source current, I_{pv} is drain-source current including photovoltaic effect only and I_{pc} is the photoconductive current in the channel region of MESFET.

The height of Schottky and back depletion regions from $y = 0$ and $y = a$ in linear region under illuminated condition can be obtained by substituting Eqn. (37-38) in Eqn. (11-12).

Later, an analytical model I-V model has been developed by including deep level traps and backgating under optically controlled conditions. Using the assumption of a uniform doping profile and a gradual channel approximation with the depletion region forming at channel-substrate junction, drain-source current in linear region can be expressed as [21]:

$$I_{pv}(x) = qZ\left(N_d - N_{sub}^-\right)\xi_x\left(a - h_{bg}^f(x) - h_{bg}^b(x)\right) \quad (40)$$

where $\xi_x\left(=-dV/dx\right)$ is electric field along the x-direction in the channel and last term represents the effective channel opening restricted by both depletion regions.

If the source and drain parasitic resistances are neglected, integrating Eqn (40) from $x=0$ to $x=L$ yields the analytical expression for the I-V characteristics in linear region.

$$I_{ds}=\frac{Z\mu_n q\left(N_d-N_{sub}^-\right)}{L}\int_0^{V_{ds}}\left(a-h_{bg}^f(x)-h_{bg}^b(x)\right)dV+I_{pc}$$
$$=A\left[3\left(\frac{V_{ds}}{V_{po}}\right)-2\left(\left(\frac{V_{ds}-V_{opgs}+f\left(V_{bg}\right)+V_{bi}}{V_{po}}\right)^{\frac{3}{2}}-\left(\frac{V_{bi}-V_{opgs}+f\left(V_{bg}\right)}{V_{po}}\right)^{\frac{3}{2}}\right)\right.$$
$$\left.-2\left(\frac{N_{sub}^-}{N_{dep}^++N_{sub}^-}\right)\left(\left(\frac{V_{ds}+V_{ch-s}-V_{opcs}}{V_{po}}\right)^{\frac{3}{2}}-\left(\frac{V_{ch-s}-V_{opcs}}{V_{po}}\right)^{\frac{3}{2}}\right)\right]+I_{pc} \tag{41}$$

where $A=\dfrac{Z\mu_n q^2\left(N_d-N_{sub}^-\right)\left(N_{dep}^+\right)a^3}{6\varepsilon_s L}$ is a constant.

Equation (41) is strictly valid up to the onset of saturation when electric field in the channel reaches saturation electric field (E_s) at $V_{ds}=V_{sat}=\left(\left(1/V_{opgs}-V_{th}\right)+\left(1/E_sL\right)\right)^{-1}$ [25].

Therefore, $I_{ds\,sat}$ at the onset of velocity saturation is $I_{ds\,sat}=I_{ds}\left(V_{ds}=V_{sat}\right)$.

In deriving Eqn. (41), we implicitly assumed that the channel length is constant. When MESFET is biased in saturation region depletion regions at drain end of gate extends laterally into the channel reducing the effective channel length. In a physical model, channel length modulation is the phenomenon producing finite output conductance in saturation region. The effective channel length of MESFET in saturation region is

$$L_{eff}=L-L_s \tag{42}$$

here $L_s=2.06\,K_d\left(\dfrac{\varepsilon_s\left(V_{ds}-V_{sat}\right)}{q\sqrt{n_{cr}}N_d}\right)^{1/2}$ is length of velocity saturation region below gate [25], K_d is a domain parameter [25] and n_{cr} is the characteristic doping density of GaAs.

Analytical expression for I-V characteristics in saturation region is, $I_{ds}=I_{ds\,sat}\left(L\rightarrow L_{eff}\right)$

$$I_{ds}=A_{eff}\left[3\left(\frac{V_{sat}}{V_{po}}\right)-2\left(\left(\frac{V_{sat}-V_{opgs}+f\left(V_{bg}\right)+V_{bi}}{V_{po}}\right)^{\frac{3}{2}}-\left(\frac{V_{bi}-V_{opgs}+f\left(V_{bg}\right)}{V_{po}}\right)^{\frac{3}{2}}\right)\right.$$
$$\left.-2\left(\frac{N_{sub}^-}{N_{dep}^++N_{sub}^-}\right)\left(\left(\frac{V_{sat}+V_{ch-s}-V_{opcs}}{V_{po}}\right)^{\frac{3}{2}}-\left(\frac{V_{ch-s}-V_{opcs}}{V_{po}}\right)^{\frac{3}{2}}\right)\right]+I_{pc} \tag{43}$$

where $A_{eff}=A|_{L\rightarrow L_{eff}}$. The first two terms in (43) are similar to the conventional analytical I-V model with gradual channel approximation and abrupt depletion layer [21]. Reduction in the drain current due to back depletion region which in turn due to the presence of deep level traps in the substrate is evident from the last term of (43). Backgating further reduces drain current by increasing the width of both depletion regions. Finally intrinsic small signal parameters like transconductance and output conductance of GaAs MESFET can be derived from the modeled I-V characteristics.

Transconductance and drain-source resistance under illuminated conditions are

$$g_m=\left.\frac{\partial I_{ds}}{\partial V_{gs}}\right|_{V_{ds}=const} \quad \text{and} \quad R_{ds}=\left.\frac{\partial V_{ds}}{\partial I_{ds}}\right|_{V_{gs}=const} \tag{44}$$

III. NUMERICAL RESULTS AND DISCUSSION

Computed photo-induced voltage across Schottky junction is presented in Fig 2(a) (dashed line) as a function of incident optical power with the device parameters in [7, 9]. The gate metal is assumed to be a semi transparent one with R_m and R_s as 0.65 and 0.2 respectively. The values of N_{EL2}, N_{SA}, N_{SD}, σ_n and σ_p

are considered as 1×10^{22} m^{-3}, 1.1×10^{21} m^{-3}, 1×10^{20} m^{-3}, $1\times10^{-18}m^2$ and $3\times10^{-18}m^2$ respectively [18]. It is observed from Fig 2(a) that the external photovoltage is increased with the increase in the incident optical power. External photovoltage with an incident optical power of $0.3\,\text{mW}$ is approximately $0.345\,\text{V}$ which is very close to the experimental value of $0.35\,\text{V}$ [9]. Variation of internal photovoltage as a function of incident optical power with the device parameters in [7, 24] is also shown in Fig 2 (a) (solid line) along with the experimental results of [24]. The value of reverse saturation current density at channel-substrate junction was estimated from [24]. It is observed that the nature is very much similar to that of external photovoltage. Larger photo absorption region in the substrate and a small reverse saturation current at channel-substrate junction makes internal photovoltage larger than external photovoltage for a given input power. The variation of photoconductive current with input optical power is depicted in Fig.2 (b) for $V_{ds}=3.5V$ and $V_{gs}=-1V$. Various parameters used in this calculation are taken from [7]. As the input power increases, depletion widths of both front and back depletion regions decrease resulting in larger photoconductive current. Photoconductive current is typically in micro-sub micro ampere range as evident from Fig 2 (b).

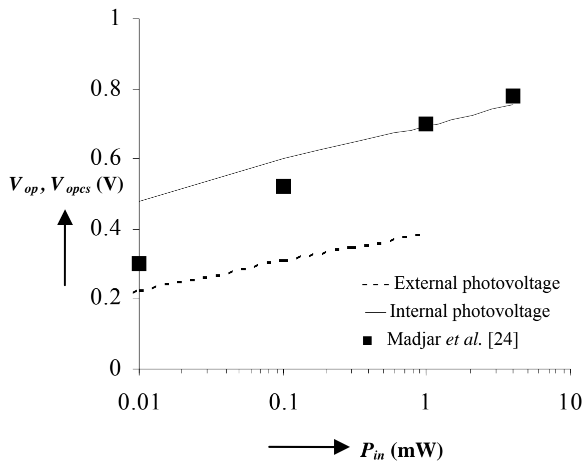

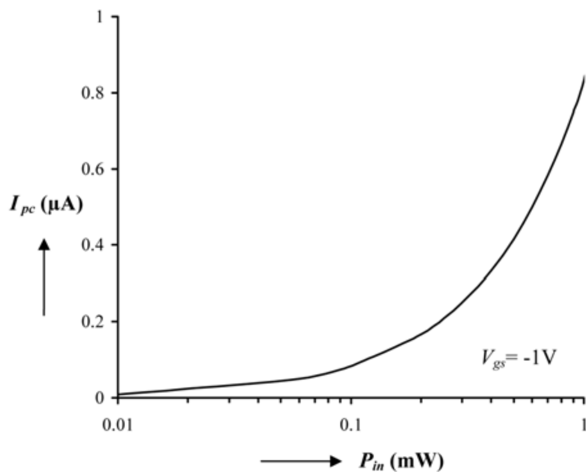

Fig. 2. Variation of (a) external, internal photovoltage as a function of optical power, (b) photoconductive current as a function of incident optical power. The results of internal photovoltage are also compared with reported experimental results [24].

Since new expressions for I-V characteristics have been derived including deep level traps in the substrate and backgating with and without illumination, it is necessary to check validity of the above-modeled expressions. To show how deep level traps in the substrate affect channel current, we simulated I_{ds}-V_{ds} characteristics without DLT (Deep Level Traps) and with DLT for $V_{gs}=0$ under dark condition and are shown in Fig 3. We validated our model with the results of numerical simulation by Son *et al.* [18]. It is observed that presence of DLT with concentration $1\text{x}10^{22}$ $/m^3$ degrades drain-source current severely. In order to investigate the effect of backgate voltage on the front

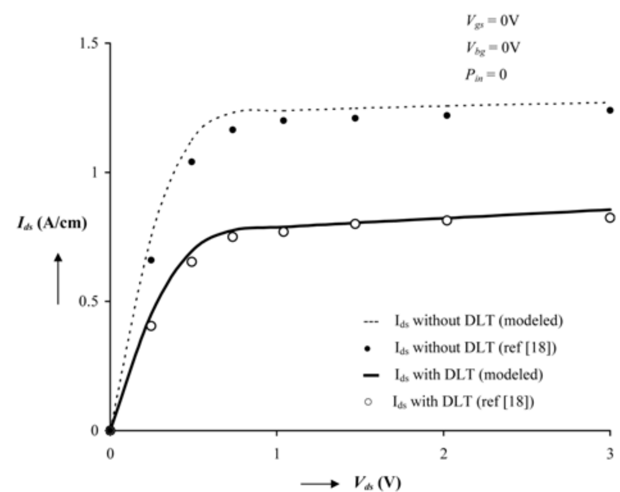

Fig. 3. I_{ds}-V_{ds} characteristics of GaAs MESFET without including DLT (dashed line) and including DLT with a concentration of N_{EL2} = $1\text{x}10^{22}$ m^{-3} (solid line). Modeled results are compared with the results of two-dimensional numerical simulation [18].

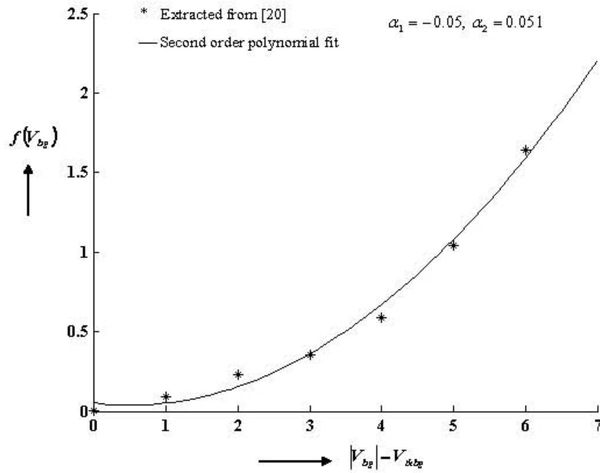

Fig. 4. Second order interpolation of $f(V_{bg})$ to include the effect of backgating through Schottky depletion modification. $f(V_{bg})$ is extracted from the measured depletion width for different backgate voltages [20] with V_{thbg} as 3V.

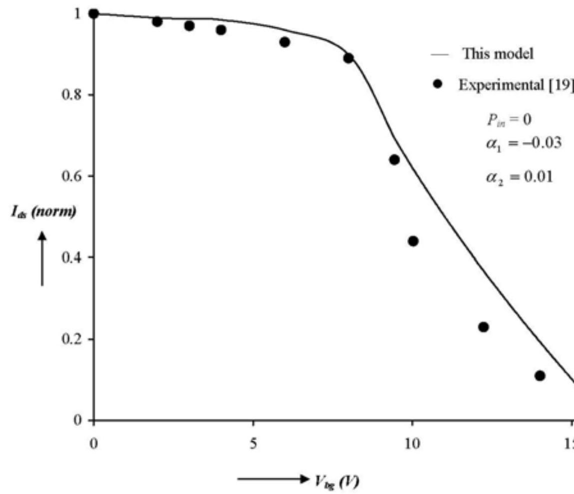

Fig. 5. Calculated dependence of normalized saturation drain current (normalized by dividing current under zero backgate bias) for GaAs MESFET on backgate voltage. Modeled normalized I_{ds} is compared with experimental result of [19]. Various parameters used in this comparison are: $a = 0.12\,\mu\text{m}$, $N_d = 2\times10^{23}\,\text{m}^{-3}$, $V_{ds} = 2.5V$, $V_{gs} = 0V$, $N_{sub} = 5\times10^{21}\,\text{m}^{-3}$, $V_{bi} = 0.7V$ and $V_{thbg} = 8V$ [19].

depletion region, we have compared the function $f(V_{bg})$ for $|V_{bg}| \geq V_{thbg}$ described by Eqn (10) to that of the experimental results in Fig 4. The experimental data has been extracted from the reported results for the variation of front depletion height with backgate voltage [20]. A good matching is observed between the two results for $\alpha_1 = -0.05$ and $\alpha_2 = 0.051$. Once α_1 and α_2 are extracted, front depletion width can be accordingly modified. Calculated dependence of backgate voltage on normalized drain-source current in saturation region has been shown in Fig 5 along with reported experimental results in literature [19] under dark condition. Sudden drop in saturated drain current beyond certain threshold voltage is reproduced. Decrease of the drain-source current is attributed to the expansions of both front and back depletion regions.

Drain-source current of GaAs MESFET under optically controlled conditions in both linear and saturation region is shown in Fig 6. Different parameters used in our model are taken from [7]. Modeled drain-source current closely tracks experimental results of [7] under dark and illuminated conditions particularly in saturation region of device operation. One can achieve better matching in linear region using a complicated velocity-field relationship rather than a simple two region model. Finite slope of I-V characteristics in saturation region is explained with the help of channel length modulation (previous models fail to account for the finite output conductance in saturation region). The effect of backgating on I-V characteristics under dark condition is also shown in the same figure. Backgate voltage greater than certain threshold voltage (V_{thbg}) modulates both depletion regions thereby reducing the drain current. A substantial increase in drain current due to illumination is observed in Fig 6. Under illuminated condition of the device excess carriers in front and back depletion regions develop photo-voltages across these depletion regions which reduce respective depletion widths thereby increasing the drain-source current. Comparing Fig 2(b) and Fig 6, photoconductive current is much smaller than the total drain-source current by several orders of magnitude. Finally, photo effects on intrinsic small signal parameters of GaAs MESFET such as transconductance and output resistance are simulated and shown in Fig 7 along with backgating and DLT effects. It was observed again that presence of DLT in substrate reduces transconductance and increases output resistance particularly near threshold voltages. Backgate voltage further reduces transcon ductance and increases output resistance. But when the device is illuminated both photovoltaic and photocon

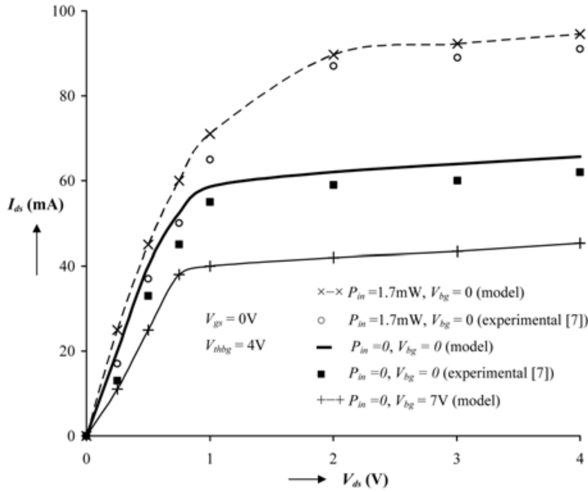

Fig. 6. Simulated I-V characteristics of GaAs MESFET under optically controlled and backgating conditions. Comparison of modeled I-V characteristics with reported experimental results [7] is also shown.

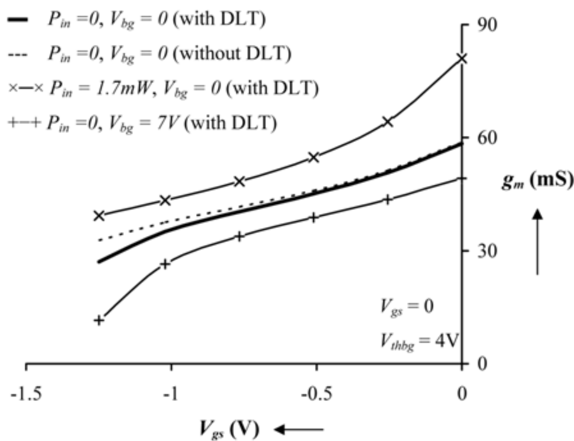

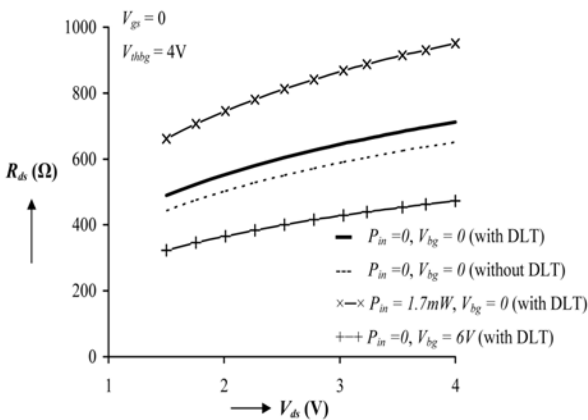

Fig. 7. Transconductance and output resistance of GaAs MESFET under dark, illuminated and backgating conditions. Deviation in transconductance and output resistance without considering DLT (ideal case), with DLT (real case) is also depicted. Various parameters in this calculation are taken from [7].

ductive effects increases transconductance and decree ases output resistance.

IV. CONCLUSIONS

A new and systematic way of modeling photo effects on the static I-V characteristics of GaAs MESFET's in both linear and saturation regions is presented. Effect of illumination on the device is explained in terms of photovoltaic and photoconductive effects. Photocon ductive current is shown to be small by several orders of magnitude than total drain-source current. Reduction of drain-source current due to deep level traps in the substrate is explained analytically under optically controlled conditions of GaAs MESFET for the first time. Finite slope in the I-V characteristics in saturation region of GaAs MESFET is modeled with the help of channel length modulation. Further, effect of backgating is also included in modeling I-V characteristics. Finally, small signal parameters of MESFET such as transconductance and output resistance are derived from the modeled I-V characteristics. The theoretical conclusions are complemented by comparing with reported experimental results in the literature, which conform the theory. Since accurate dc modeling is key to accurate ac modeling, we believe that this model may be very useful for the designing of GaAs MESFET's particularly in MMIC's and OEIC's.

REFERENCES

[1] A. J. Seeds, "Microwave photonics," *IEEE Trans Microwave Theory Tech.*, vol. 50, no. 3, pp.877-887, March 2002.

[2] S. J. Rossek and C.E. Free, "Optical control of microwave signals using GaAs FETs," *IEE Electron. Commun. Eng. J.*, vol.6, no. 1, pp.21-30, February 1994.

[3] J. Rodriguez-Tellez *et al.* "Optically controlled 2.4GHz MMIC Amplifier," *Proc. of 10th International Conference on Electronics, Circuits & Systems (ICECS)*, pp.970-973, December 2003.

[4] S. Kawasaki, H. Shiomi and K. Matsugatani, "A novel FET model including an illumination-

intensity parameter for simulation of optically controlled millimeter-wave oscillators," *IEEE Trans Microwave Theory Tech*, vol. 46, no.6, pp. 820-828, June 1998.

[5] S. Jit and B. B. Pal, "A new Optoelectronic Integrated Device for Light-Amplifying Optical Switch (LAOS)," *IEEE Trans. Electron Devices*, vol. 48, no.12, pp. 2732-2739, December 2001.

[6] J. F. Ahadian *et al.*, "Practical OEIC's based on the monolithic integration of GaAs–InGaP LED's with commercial GaAs VLSI electronics," *IEEE J. Quantum Electron.*, vol. 34, no.7, pp.1117-1123, July 1998.

[7] A. A. De Salles, "Optical control of GaAs MESFET's," *IEEE Trans. Microwave Theory Tech.*, vol. 31, no.10, pp.812-820, October 1983.

[8] R. N. Simons, "Microwave performance of an optically controlled AlGaAs/GaAs high electron mobility transistor and GaAs MESFET," *IEEE Trans. Microwave Theory Tech.*, vol. 35, no.12, pp.1444-1455, December 1987.

[9] J. L. Gautier, D. Pasquet, and P. Pouvil, "Optical effects on the static and dynamic characteristics of a GaAs MESFET," *IEEE Trans. Microwave Theory Tech.*, vol.33, no.9, pp.819-822, Septem ber 1985.

[10] R. N. Simons and K. B. Bhasin, "Analysis of Optically controlled microwave/ millimeter-wave device structures," *IEEE Trans Microwave Theory Tech*, vol.34, no.12, pp.1349-1355, December 1986.

[11] V. K. Singh and B. B. Pal, "Effect of optical radiation and surface recombination on the RF switching parameters of a GaAs MESFET," *IEE Proc. Optoelectron.*, vol.137, no.2, pp. 124-128, April 1990.

[12] P. Chakrabarti, A. Gupta, and N. A. Khan, "An analytical model of GaAs OPFET," *Solid State Electron.*, vol. 39, no.10, pp.1481-1490, October 1996.

[13] S. H. Lo and C. P. Lee, "Numerical analysis of the photo effects in GaAs MESFET's," *IEEE Trans. Electron Devices,* vol.39, no.7, pp.1564-1570, July 1992.

[14] N. P. Khuchua *et al.*, "Deep-Level effects in GaAs Microelectronics: A Review," *Russian Microelectronics*, vol.32, no.5, pp.257-274, 2003.

[15] J. F. Wager and A. J. McCamant, "GaAs MESFET interface considerations," *IEEE Trans. Electron Devices,* vol. 34, no.5, pp. 1001-1007, May 1987.

[16] F. Gao *et al.*, "Sidegating effect in ion-implanted GaAs self-aligned gate MESFET MMICs," *Proc. of GaAs Reliability workshop*, pp.27-35, Novem ber 1998.

[17] E. B. Stoneham, P. A. J. O'Sullivan, S. W. Mitchell and A. F. Podell, "Working with nine different foundries", Proc. of *GaAs Integrated Circuit (GaAs IC) Symposium Tech Digest*, pp.11-14, October 1990.

[18] I. Son and T. W. Tang, "Modeling deep-level trap effects in GaAs MESFET's," *IEEE Trans. Electron Devices*, vol. 36, no.4, pp.632-640, April 1989.

[19] Y. H. Chen, Z. G. Wang, J. J. Qian and M. F. Sun, "Threshold behavior in backgating in GaAs metal-semiconductor field effect transistors: Induced by limitation of channel-substrate junction to leakage current," *J. Appl. Phys.*, vol.81, no.1, pp.511-515, January 1997.

[20] J. Wu, Z.G. Wang, T. W. Fan, L. Y. Lin and M. Zhang, "Sidegating effect on Schottky contact in ion-implanted GaAs," *J. Appl. Phys.*, vol. 78, no.12, pp.7422-7423, December 1995.

[21] S. M. Sze, *Physics of Semiconductor Devices*, Wiley, New Delhi, 1999.

[22] A. H. Khalid and A. A. Rezazadeh, "Fabrication and characterization of transparent gate field effect transistors using indium tin oxide," *IEE Proc. Optoelectron.*, vol.143, no.1, pp. 7-11, February 1996.

[23] T. Minami, "Transparent conducting oxide semiconductors for transparent electrodes," *Semicond. Sci. Technol.*, vol.20, no.4, pp. S35-S44, April 2005.

[24] A. Madjar, P. R. Herczfeld and A. Paolella, "Analytical model for optically generated currents in GaAs MESFETs," *IEEE Trans. Microwave Theory Tech*, vol. 40, no.8, pp.1681-1691, August 1992.

[25] Michael Shur, *GaAs Devices and Circuits*, Plenum press, New York, 1986.

Neti V.L. Narasimha Murty was born in the East Godavari District of Andhra Pradesh, India, in 1981. He has received his B. Tech degree in Electronics & Communications En gineering from Jawaharlal Nehru Technological University (JNTU), Andhra Pradesh, India in April 2002. He is presently working towards his PhD degree in the Department of Electronics Engin eering, Institute of Technology, Banaras Hindu Univer sity (IT-BHU), and Varanasi, India.

He is a Senior Research Fellow in the same department. His present research interests include characterization of microwave-photonic devices, defect levels in semi-insulating substrates and high-speed devices.

S. Jit was born in the Midnapore district of West Bengal, India in 1970. He received the B. E. degree from the Bengal Engineering Coll ege of the University of Calcutta, West Bengal, in 1993; M. Tech from the Indian Institute of Technology, Kanpur in 1995; and Ph.D. degree from the Institute of Technology, Banaras Hindu University (IT-BHU), Varanasi, India in 2002. From 1995 to 1998, he has worked as Lecturer in the Department of Electronics and Communications Engineering of the G. B. Pant Engineering College, Pauri-Garhwal, Uttar Pradesh (presently Uttaranchal), India. He joined the Department of Electronics Engineering, IT-BHU as Lecturer in 1998. Since 2001, he has been working as Senior Lecturer in this department. Dr. Jit has published more than 25 research papers in international journals and conference proceedings. He is the recipient of the INSA (Indian National Science Academy) Visiting Fellowship for the year 2006-2007. His research interests include the modeling and simulation of short-channel FET's, optical bistability and switching using III-V semiconductors, quantum-well infrared photodetectors and optically controlled microwave devices and circuits. Dr. Jit is a life Member of the Institution of Electronics and Telecommunication Engineers (IETE), India.